ISSN 1070-3632, Russian Journal of General Chemistry, 2015, Vol. 85, No. 4, pp. 959–973. © Pleiades Publishing, Ltd., 2015.

Complexation Modulated Redox Behavior of Transition Metal Systems (Review)[1]

Masood Ahmad Rizvi

Department of Chemistry, University of Kashmir, Srinagar, Kashmir, 190006 India
e-mail: masood_ku2@yahoo.com

Received September 29, 2014

Abstract—Ligand effect is a favorable factor in modulation of redox potential of transition metal ion oxidation-reduction systems. Coordination promoted redox action of transition metals can be an efficient approach to design of new redox systems with specific applications. The current review is devoted to the complexation effect of selected ligands on the redox potential of iron, cobalt and copper redox couples and application of such systems in analytical estimations. Indirect estimation of non redox systems by a non redox reaction over a platinum electrode has been referred to as a pseudo indicator action. Application of coordination modulated redox potentials in the natural attenuation of toxic environmental contaminants is also presented.

Keywords: redox potential, ligand effect, iron transport; 1, 10-phenanthroline, neocuproine, desferrioxamine, nitroaromatic reduction

DOI: 10.1134/S1070363215040337

Complexation effect on redox potential. Redox systems with tailor made potentials are desired for applications in artificial photosynthetic reactions [1], fuel cell catalysts solar energy conversions [2], hydrogen production and bio-memitic chemistry [3]. Complexation with an appropriate ligand can modulate the redox potential of transition metals redox couples beyond the natural range [4, 5]. The complexation effect on redox potential can be explained by specific stabilization of transition metal oxidation states in a redox couple. The complexation effect on redox potential can be rationalized using the thermochemical cycle (Scheme 1) [7, 8]. The ligand effect is the promising phenomenon in the design and development of redox potentials with desired applications [6].

$$\Delta G_1 + \Delta G_2 = \Delta G_3 + \Delta G_4, \tag{1}$$

$$\Delta G_1 = -nFE_{\text{aqua}};\ \Delta G_2 = -RT\ln \beta^{\text{II}},$$

$$\Delta G_3 = -RT\ln \beta^{\text{III}};\ \Delta G_4 = -nFE_{\text{complex}},$$

$$\Delta G_4 = (\Delta G_1 + \Delta G_2) - \Delta G_3, \tag{2}$$

$$-nFE_{\text{complex}} = -nFE_{\text{aqua}} + \frac{RT}{nF}\ln\frac{\beta^{\text{III}}}{\beta^{\text{II}}},$$

$$E_{\text{complex}} = E_{\text{aqua}} - \frac{RT}{nF}\ln\frac{\beta^{\text{III}}}{\beta^{\text{II}}}. \tag{3}$$

According to Eq. (3) the ratio of formation constants $\beta^{\text{III}}/\beta^{\text{II}}$ modulates the redox potential of a redox couple in complexes. With the proper adjustment of the ratio the redox potential can be tuned to any desired value. Thus the electrochemical behavior of transition metals ions is also modified by the complexation effect which leads to a different reduction potential in the complexed state compared to the free state [Eq. (3)]. The complexation effect on redox potentials helps to understand mechanisms of the natural redox processes [9],

Scheme 1. Thermochemical cycle for complexation effect on redox potential.

$$\begin{tikzcd}
\mathrm{M}^{3+}_{\text{aqua}} \arrow[r, shift left, "\Delta G_1"] \arrow[d, shift left, "nL"] & \mathrm{M}^{2+}_{\text{aqua}} \arrow[l, shift left, "e^-"] \arrow[d, shift left, "nL"] \\
\mathrm{M}^{3+}_{\text{complex}} \arrow[r, shift left, "\Delta G_4"] \arrow[u, shift left, "\Delta G_3"] & \mathrm{M}^{2+}_{\text{complex}} \arrow[l, shift left, "e^-"] \arrow[u, shift left, "\Delta G_2"]
\end{tikzcd}$$

---

[1] The text was submitted by the author in English.

Scheme 2. Structure of phenanthrene moiety, Phen ligand and $[Fe(phen)_3]^{2+}$ complex.

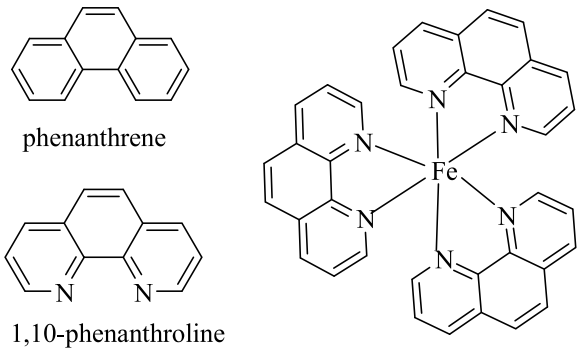

action of metalloenzymes, metals extraction by siderophores [10] and prevention of unwanted biological oxidation [11].

Design and development of novel redox systems. Transition metals have multiple oxidation states separated by a finite potential value. A pair of transition metal oxidation states forms a redox couple with the fixed redox potential. Modification of redox properties of transition metals ions allows to use the new systems in specific areas such as photoelectro chemical and redox flow cells, electrochemical reaction initiation, microbiological fuel cells, electron acceptors for hydrogen production, and electro catalysis [12]. Ligand effect on redox potentials paves a valuable way for design and development of redox systems for analytical monitoring of transition metals ions and their mixtures [13].

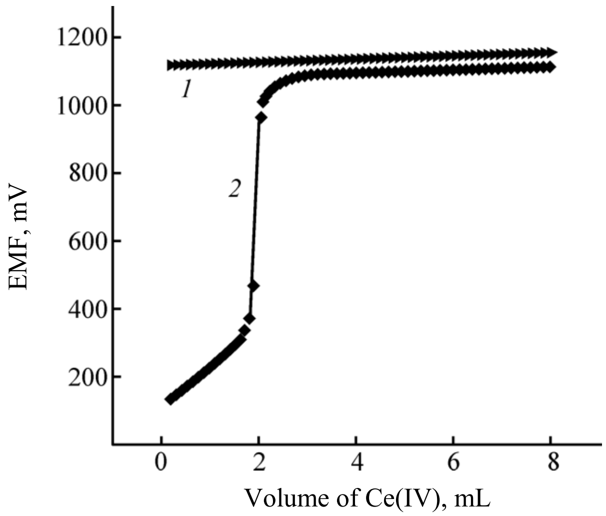

Fig. 1. Potentiometric response of Co(II) oxidation with Ce(IV) (*1*) in absence and (*2*) in presence of the Phen ligand.

Iron 1,10-phenanthroline system. 1,10-Phenanthroline (Phen) is a strong pi acceptor type bidentate ligand with two nitrogen donor sites in the aromatic phenanthrene structure (Scheme 2). The Phen ligand forms octahedral complexes in aqueous solutions with transition metals.

The Phen ligand forms complexes of different stabilities with two oxidation states (2+ and 3+) of iron [8, 14]. Theoretical analysis of iron Phen complexes reveals a charge transfer absorption band involving π electron migration from the *d*–π (t_{2g} type) orbitals of iron (HOMO) to the lowest vacant π* molecular orbital of the Phen ligand (LUMO).This electron migration between metal HOMO and ligand LUMO is considered to be of stabilizing nature as is evident from the higher formation constant of Fe(II)Phen complex ($\log \beta^{III} = 21.3$) over Fe(III)Phen complex ($\log \beta^{III} = 14.1$) [8]. The most desirable condition for this *d*π–*p*π type electron transfer is diamagnetic, lower charge density octahedral, low spin t_{2g}^6 configuration (due to π symmetry) of the metal which allows maximum electron transfer from metal HOMO to ligand LUMO. The higher stabilization of Fe(II) by Phen ligand increases the reduction tendency of Fe(III) to Fe(II) which enhances the reduction potential of Fe(III)–Fe(II) redox couple from 0.771 to 1.14 V (vs SHE) [15, 16]. The Phen modulated redox potential of Fe(III)–Fe(II) redox couple was observed by the changes in the potentiometric response of Fe(II)–Ce(IV) redox process in absence and in presence of Phen ligand [13].

In potentiometric titration of Co(II)–Fe(II) binary mixture with Ce(IV) a single equivalence point was observed in absence of Phen ligand while in presence of it two equivalence points attributed to the molar amounts of Fe(II) and Co(II) in the mixture were observed. Thus the Phen ligand removed the interference in simultaneous estimation of Co(II) and Fe(II) binary mixture with Ce(IV) [13].

Cobalt 1,10-phenantroline (Phen) system. Different oxidation states of transition metals are electronically equivalent and are often grouped in a d^n system. Fe(II) and Co(III) belong to d^6 system and are similar in action towards the Phen ligand. However Phen modification of the redox potential in case of Co(III)–Co(II) redox couple is inverse to that of Fe(III)–Fe(II) redox couple. This is due to higher Phen stabilization of Co(III) than Co(II) which diminishes the reducing tendency of Co(III) and, hence, decreases the redox potential of Co(III)–Co(II) redox couple contrary to

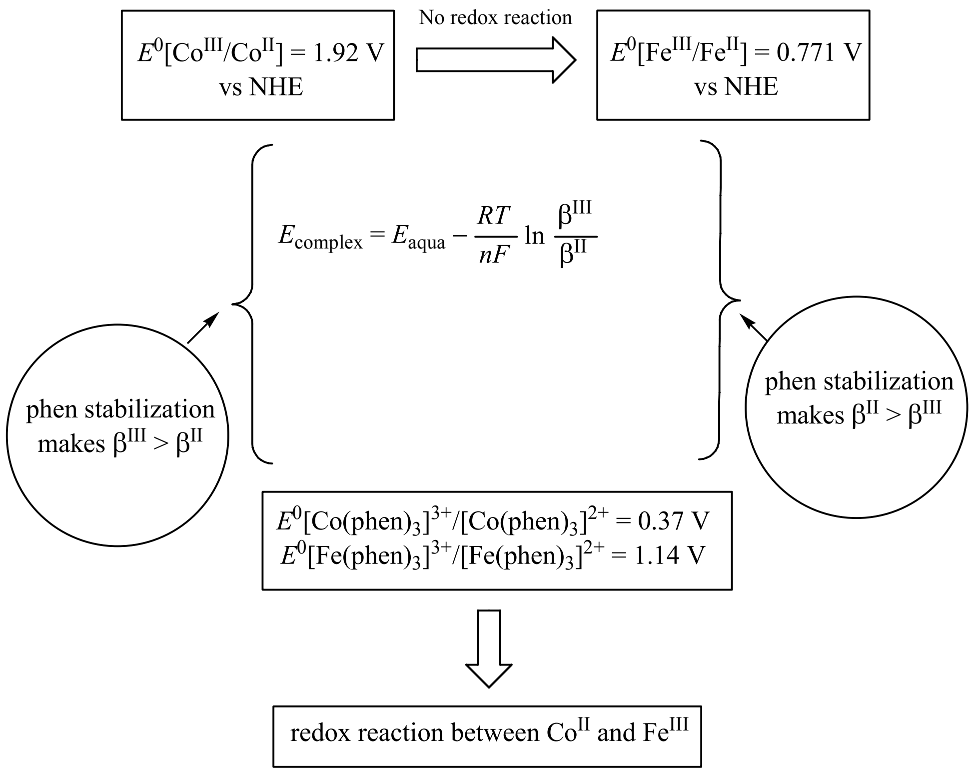

Fig. 2. 1,10-Phenanthroline (Phen) ligand effect on redox behavior of cobalt and iron.

the increase of redox potential in case of Fe(III)–Fe(II) redox couple [Eq. (3)]. The Phen modified redox potential of Co(III)–Co(II) redox couple has been explored in removing the non-spontaneity of Co(II) oxidation with Ce(IV) (Fig. 1) [17].

Absence of any potential jump in potentiometric titration of Co(II) with Ce(IV) is due to mismatch of redox potential [Ce(IV)–Ce(III) = 1.74 V and Co(III)–Co(II) = 1.92 V]. Hence a redox reaction involving oxidation of Co(II) to Co(III) and reduction of Ce(IV) to Ce(III) is not feasible. The unfavorable redox reaction of metal ions $M^{ox} + N^{red} \leftrightarrow M^{red} + N^{ox}$ can take place in presence of a suitable ligand which forms more stable complex either with M^{ox} rather than M^{red} or N^{ox} rather than N^{red}. This effect of a ligand in stabilizing one of two forms of the redox couple results in a different reduction potential in the complexed state compared to the free state or that in hydrated state. The complexes that favor stabilization of metals in the oxidized form would make the reduction potential lower than in hydrated form. On the contrary the complexes that stabilize metals in the reduced form would raise the reduction potential compared to that of the hydrated form. 1,10-Phenanthroline forms the octahedral complex with Co(II) that is more stable than Co(III) complex and remarkably decreases its reduction potential of aqueous state value from 1.92 to 0.652 V [15]. The comparison of aqueous state potentials suggests that the direct oxidation of Co(II) with Ce(IV) is not possible. However, lowering the potential by complexation with 1,10–phenanthroline can make this redox reaction feasible (Fig. 1). Stabilization of Co(III) by the Phen ligand is due to the higher degree of back donation from t_2g^6 configuration, favoring $d\pi$—π^* electron delocalization [8].

Effect of Phen ligand on Fe(III)–Co(II) redox reaction. The redox reaction involving oxidation of Co(II) to Co(III) and reduction of Fe(III) to Fe(II) is not possible due to mismatch in redox potentials [18]. The aqueous redox potentials of Fe(III)–Fe(II) and Co(III)–Co(II) redox couples are 0.771 and 1.92 V respectively that do not allow the reduction of Fe(III) by Co(II). Since the Phen ligand stabilizes low spin d^6 octahedral systems with t_2g^6 configuration, it stabilizes Fe(II) more readily than Fe(III) and Co(III) more than Co(II) (Fig. 2). This leads to lower formal redox potential of Co(III)–Co(II) ($E^0[Co(phen)_3]^{3+}/[Co(phen)_3]^{2+}$ 0.37 V) and makes higher the formal potential of Fe(III)–Fe(II) ($E^0[Fe(phen)_3]^{3+}/[Fe(phen)_3]^{2+} = 1.14$ V) relative to their free (aqua) state potentials [15].

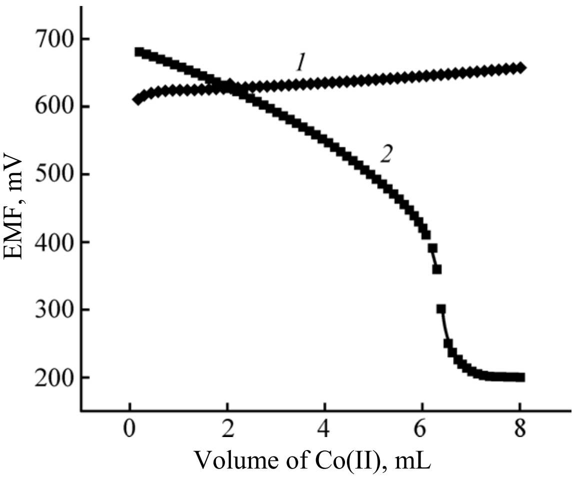

Fig. 3. Potentiometric response of Fe(III) reduction by Co(II) (*1*) in absence and (*2*) in presence of the Phen ligand.

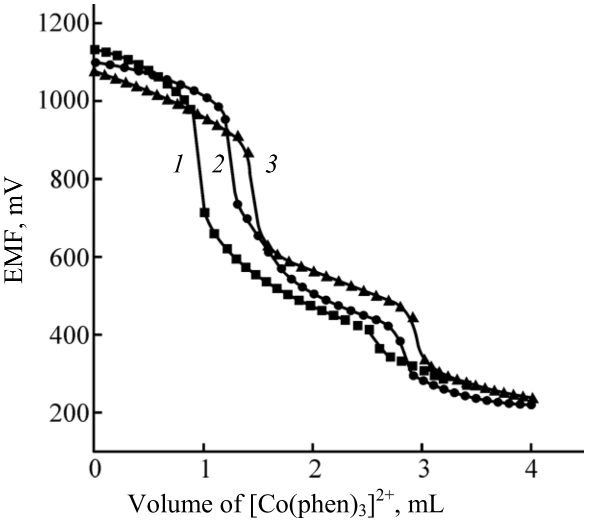

Fig. 4. Potentiometric titration of Ce(IV) and Fe(III) with Co(II) in presence of the Phen ligand. (*1*) Fe(II), 25 mL, 8×10^{-4} mol/L; Fe(III), 25 mL, 4×10^{-4} mol/L; (*2*) Fe(II) 25 mL, 6×10^{-4} mol/L; Fe(III), 25 mL, 6×10^{-4} mol/L; (*3*) Fe(II), 25 mL, 4×10^{-4} mol/L; Fe(III), 25 mL, 8×10^{-4} mol/L. Titration conditions: Ce(IV), 25 mL, 1.6×10^{-3} mol/L; Co(II), 2×10^{-2} mol/L; pH = 1.29; $T = 50°C$; L/M ratio = 12.5.

Upon Phen modulation of cobalt and iron redox potentials the redox reaction involving oxidation of Co(II) by Fe(III) becomes feasible as can be seen from the potentiometric titration plot (Fig. 3).

Phen modulated redox potentials for simultaneous iron oxidation state analysis. Simultaneous determination of iron oxidation states is essential in biological and environmental chemistry. Environmentally benign analytical methods with high versatility, selectivity, sensitivity, precision, and reproducibility are always desired. Such method utilizing 1,10-Phenanthroline modulated redox potentials of iron and cobalt was proposed for benign iron speciation analysis by Rizvi and coauthors [8]. It is based on the Phen modulated redox potential of cobalt and iron which allow the simultaneous reduction of Ce(IV) and Fe(III) by Co(II) without any interference. The concept was utilized in a simple potentiometric redox back titration with standardized Ce(IV) as an excess reagent which oxidized Fe(II) to Fe(III) in a preliminary to titration step.

The $[Co(Phen)_3]^{2+}$ titrant first reduced unreacted Ce(IV) to Ce(III) and then $[Fe(Phen)_3]^{3+}$ to $[Fe(Phen)_3]^{2+}$. The plot of EMF and volume of $[Co(Phen)_3]^{2+}$ displayed two clear inflection points (Fig. 4).

The first endpoint corresponds to the molar amount of free Ce(IV) in the mixture. The second end point corresponds to the equivalence of total iron. On the basis of these data the amounts of Fe(II) in the mixture and the initial Fe(III) were deduced. No potential jump was observed in absence of Phen but two clear inflections corresponding to the molar amounts of Fe(II) and Fe(III) were observed at L/M ratio higher than 10. The free energy change (potential change) at the equivalence point also got enhanced with increase in concentration of the Phen ligand [Fig. 5, Eq. (4)] [19].

$$E_{\text{complex}} = E_{\text{aqua}} + \frac{2.303RT}{nF}\log\beta + \frac{2.303RT}{nF}\log\,[\mathrm{ML}_n]^{n+}. \tag{4}$$

The effect of Phen complexation was also demonstrated by the change in the potentiometric behavior of redox titration under different pH (Fig. 6) [9].

pH had a multidimensional influence on the redox reaction: very low pH (<1) was inappropriate for Phen complexation with metals, higher pH (>3) disfavored stability of Co(II)Phen complex. Much higher pH (> 5.0) resulted in precipitation of Ce(IV) and Fe(III)

Scheme 3.

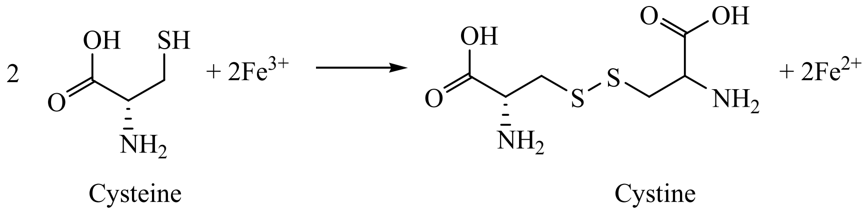

giving a suspension. The pH range of 1–2 represented the optimum combination of pH based factors [17].

Comparative ligand effect on Fe(III)–cysteine redox reaction. The reaction of cysteine with Fe(III) is an overall one-electron-transfer process that involves the reduction of Fe(III) to Fe(II) accompanied by oxidation of cysteine to cystine (Scheme 3).

Aqueous phase electron transfer between Fe(III) and cysteine is not feasible due to mismatch of redox potentials. However, upon complexation of Fe(III) with ligands having higher Fe(II) formation constants than Fe(III), Fe(III) cysteine redox reaction takes place. The coordination of Fe(II) stabilizing ligand increases iron redox potential [Eq. (3)] and makes Fe(III) cysteine redox reaction spontaneous. Potentiometric titration of Fe(III) with cysteine [20] displayed the potential jump at the equivalence point only in presence of the ligand and ca 50°C. Potential change in the vicinity of the inflection point was found to be proportional to stability of Fe(II) complex with the selected ligands (Fig. 7).

Scheme 4. Coordination coupled electron transfer between Fe(III) and cysteine.

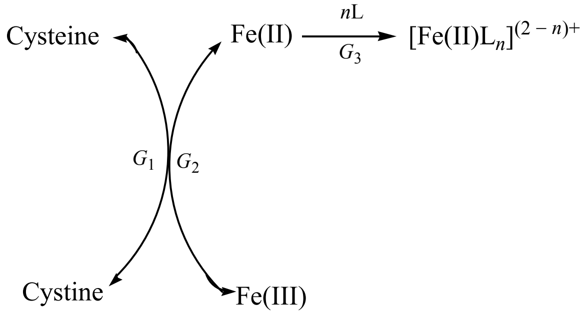

L = *a* = ETDA, *b* = aqua, *c* = Terpy, *d* = Bipy, *e* = Phen

$$\Delta G_{rxn} = (G_3 + G_2) - G_1$$

$$G_3 = -2.303RT\log\beta^{\mathrm{II}},\ \beta^{\mathrm{II}} = a < b < c < d < e$$

Distinctive influence of the ligands under study on potentiometric behavior of Fe(III) cysteine redox reaction can be explained by coordination coupled electron transfer (Scheme 4).

In presence of the ligand free energy of the complexation step G_3 adds to free energy of electron transfer (step G_2) leading to an overall free energy

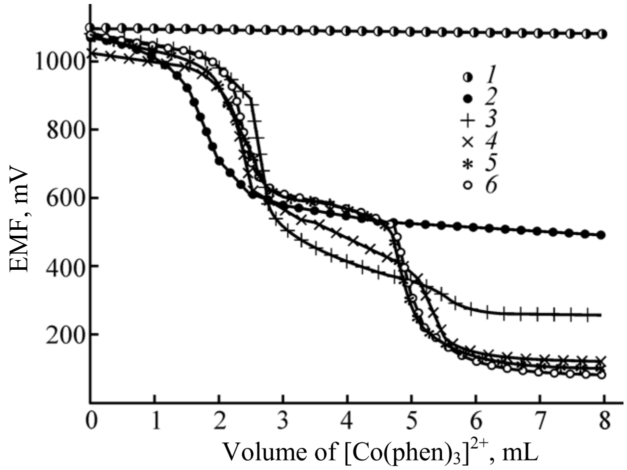

Fig. 5. Potentiometric titration of Ce(IV) and Fe(III) mixture with Co(II) in presence of increasing Phen ligand concentration: (*1*) 0.00, (*2*) 1.42, (*3*) 3.58, (*4*) 7.14, (*5*) 14.28, and (*6*) 17.85.

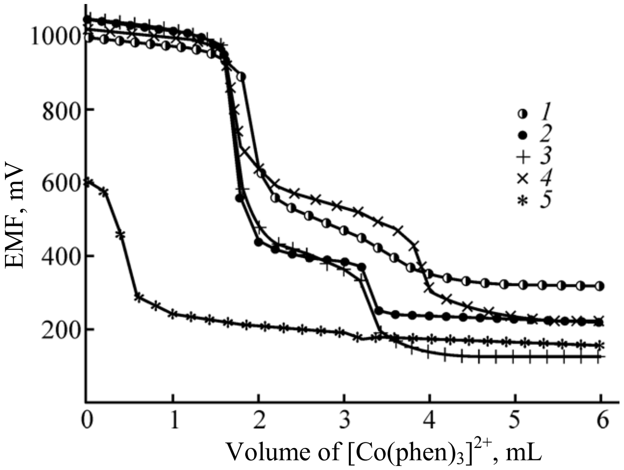

Fig. 6. Potentiometric titration of Ce(IV) and Fe(III) mixture with Co(II) in presence of the Phen ligand at different pH: (*1*) 0.14, (*2*) 1.09, (*3*) 1.69, (*4*) 3.92, and (*5*) 5.00.

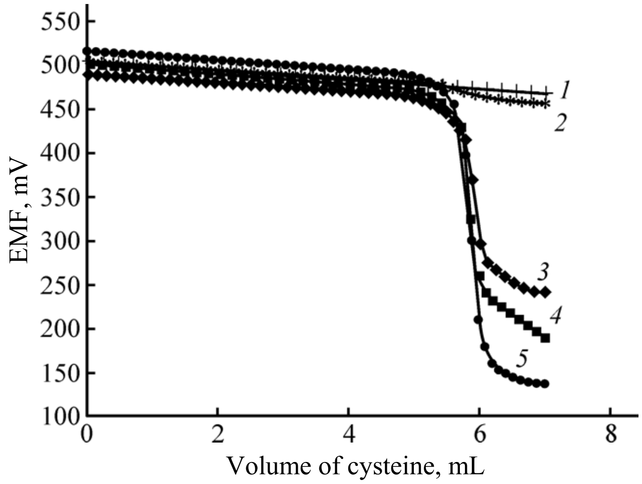

Fig. 7. Potentiometric titration of Fe(III) with cysteine in presence of different ligands systems: (*1*) EDTA, (*2*) H_2O, (*3*) TerPy, (*4*) BiPy, and (*5*) Phen.

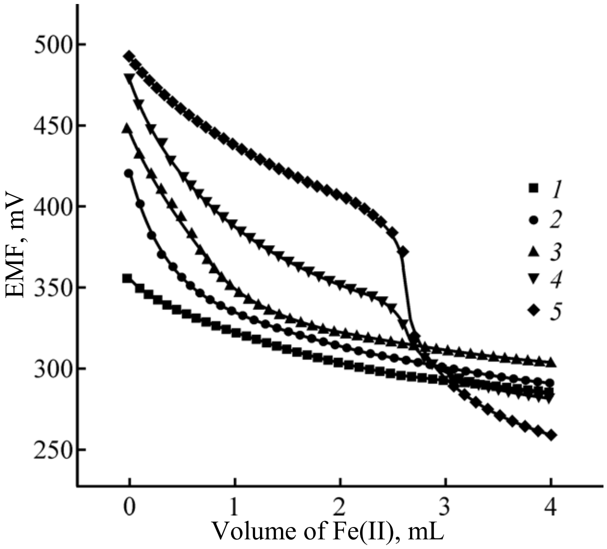

Fig. 8. Potentiometric titration of Cu(II) with Fe(II) in presence of different NC ligand molar amounts, mM: (*1*) 10, (*2*) 20, (*3*) 40, (*4*) 60, and (*5*) 80.

change of the reaction to be $(G_3 + G_2) - G_1$, compared to $G_2 - G_1$ in absence of a ligand. The strength of Fe(II) complex (β^{II} value) contributes to the G_3 component of the overall free energy change of the reaction. Higher Fe(II) formation constant of the ligand makes higher its contribution to G_3 and free energy change of the reaction (larger change in EMF) at equivalence [10].

Copper neocuproine (NC–2,9-dimethyl-1,10-phenanthroline) system. Redox reaction of Fe(II) with Cu(II) in aqueous media is thermodynamically non spontaneous. However, in presence of 2,9-dimethyl-1,10-phenanthroline, also known as Neocuproine (NC), Fe(II)–Cu(II) redox reaction becomes feasible (Fig. 8).

NC as a ligand stabilizes Cu(I) more than Cu(II) and hence Cu(II)–Cu(I) reduction potential increases in presence of the NC ligand to facilitate electron transfer from Fe(II) to Cu(II). NC modulated redox potential of copper redox couple can be quantified using Eq. (5):

$$E[\mathrm{Cu(NC)_2}]^{n+} = E_{\mathrm{aqua}}(\mathrm{Cu}) - (59.16\ \mathrm{mV})\log\frac{\beta[\mathrm{Cu^{II}(NC)_2}]^{2+}}{\beta[\mathrm{Cu^{I}(NC)_2}]^{+}}. \quad (5)$$

Substituting stability constant values of Cu(II) and Cu(I) NC complexes ($\log \beta^{II} = 11.7$ and $\log \beta^{I} = 19.1$) [21] makes the reduction potential of Cu(II)–Cu(I) couple increase from 153 to 709 mV in presence of NC. In the potentiometric titration potential values were fluctuating and became stable within 1 min of the titrant addition indicating slow electron transfer which can be attributed to significant changes in coordination geometry in the course of reduction of $[\mathrm{Cu(NC)_2}]^{2+}$ to $[\mathrm{Cu(NC)_2}]^{+}$. Cu(II) complexes are known to exist in distorted octahedral configuration (Jahn Teller stabilization) while Cu(I) complexes have a tendency to form four coordinate tetrahedral structures. Thus, in the reduction reaction geometry transformation slows down the rate of electron transfer. Raashid and coauthors [21] reported the spectrophotometric study of kinetics and mechanism of NC assisted Fe(II)–Cu(II) process in which the absorbance time plot indicated electron transfer completion in ca 120–130 s [11]. The concentration effect on kinetic profile study justified the pseudo 2nd order kinetics with respect to the NC ligand and first order kinetics with respect to both Cu(II) and Fe(II). The temperature effect on kinetics revealed an overall activation barrier of 26.22 kJ $\mathrm{mol^{-1}}$ for electron transfer process. Based on spectrophotometric studies three possible mechanisms of the process can be considered.

a. Complexation of NC to Fe(II) followed by electron transfer to Cu(II)aqueous.

b. Complexation of NC to Cu(II) followed by electron transfer to Fe(II)aqueous.

c. Aqueous state electron transfer followed by complexation/stabilization by NC ligand.

Spectrophotometric plots of Fe(II) and Cu(II) in presence of NC ligand rule out the possibility of Fe(II)

NC complexation, hence removing the possibility of iron complexation *a*. Lack of potential jump in absence of the NC ligand and aqueous state redox potentials of Cu(II) and Fe(II) rule out the possibility of aqueous state electron transfer followed by NC complexation/stabilization. Thus, the most probable mechanism of Fe(II)–Cu(II) redox reaction involves complexation of Cu(II) with NC to form the less stable $[Cu(NC)_2]^{2+}$ (log β 11.7) precursor complex which gets reduced by aqueous Fe(II) to more stable $[Cu(NC)_2]^+$ (log β 19.1) and itself oxidizes to Fe(III) as follows:

$$Cu^{2+}_{aqua} + 2NC \xrightarrow{fast} [Cu(NC)_2]^{2+},$$

$$[Cu(NC)_2]^{2+} + Fe^{2+}_{aqua} \xrightarrow{k} [Cu(NC)_2]^{2+} + Fe^{3+}_{aqua}$$

$$K_{eq} = \frac{[Cu(NC)_2]^{2+}}{[Cu^{2+}][NC]^2},$$

$$[Cu(NC)_2]^{2+} = K_{eq}[Cu^{2+}][NC]^2,$$

$$\text{rate} = k[Cu(NC)_2]^{2+}[Fe^{2+}],$$

$$\text{rate} = kK_{eq}[Cu^{2+}][NC]^2[Fe^{2+}],$$

$$\text{rate} = k'[Cu^{2+}][NC]^2[Fe^{2+}].$$

Such mechanism fits in the observed 2nd order kinetics of the NC ligand and first order kinetics of Cu(II) and Fe(II). The experimentally determined average value of k was equal to 3.37 ± 0.05 dm^3 mol^{-1} s^{-1} [21].

Non redox systems over platinum electrode using iron complexes as a redox couple. Platinum is one of the most commonly used indicator electrodes with desirable surface characteristics, quick equilibration and good Nernstian behavior. An analyte which generates a redox couple in a potentiometric cell can be analyzed over Pt electrode. However, there are a number of biologically and environmentally important species like Zn^{2+}, Cu^{2+}, Ni^{2+}, Cd^{2+}, Pb^{2+}, Al^{3+}, that being non-redox (having only one stable aqueous oxidation state) fail to generate a redox couple [22]. Syed and co-authors [23] proposed the term "pseudo-indicator action" for the indirect estimation of such non redox systems over Pt electrodes. Under pseudo-indicator action a non redox analyte is indirectly estimated via its non redox reaction with one of the species in a redox couple (generated in solution) which changes the concentration of the redox couple [23]. Zn^{2+} ions are indirectly estimated over platinum electrodes using the $\{[Fe(CN)_6]^{3-}–[Fe(CN)_6]^{4-}\}$ redox couple.

$$3Zn^{2+} + 2K_4[Fe(CN)_6] \rightarrow K_2Zn_3[Fe(CN)_6]_2 + 6K^+.$$

This non redox (complexation reaction) changes the concentration of ferrocyanide in the ferricyanide–ferrocyanide redox couple.

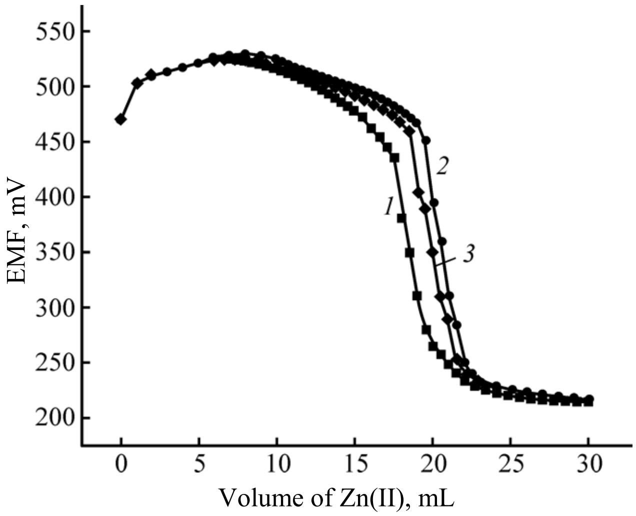

Fig. 9. Potentiometric estimation of Zn^{2+} over Pt electrode using ferricyanide-ferrocyanide redox couple, mM: (*1*) 1.3, (*2*) 1,4, and (*3*) 1.5.

Upon addition of Zn^{2+} the $[Fe(CN)_6]^{4-}$ ions are consumed which makes E_{Pt} to decrease.

Estimation of transition metal ions and their binary mixture over platinum electrode using the pseudo-indicator action of $[Fe^{III}EDTA]^-–[Fe^{II}EDTA]^{2-}$ redox couple generated in solution was studied [24]. Iron EDTA redox couple got generated in solution upon initial addition of small amount of Fe(II) to the analyte solution followed by titration with Fe(III). The analytical method uses back titration of excess EDTA with Fe(III) solution. The analyzed metal ions exhibited three types of potentiometric behavior depending upon their binding constant with EDTA ligand.

a. Single equivalence point corresponding to free EDTA was observed only in case of metals that had binding constants with EDTA ligand higher than Fe(III) and hence did not exchange the bound EDTA with Fe(II) (Fig. 10).

b. Two equivalence points assigned to free EDTA and complete exchange of metal bound EDTA to Fe(III) were observed in cases of metals characterized by binding constants with EDTA lower than Fe(III) (Fig. 11).

c. Single stoichiometric equivalence assigned to total EDTA added was observed in cases of metals characterized by very low binding constant with EDTA compared to Fe(III) (Fig. 12).

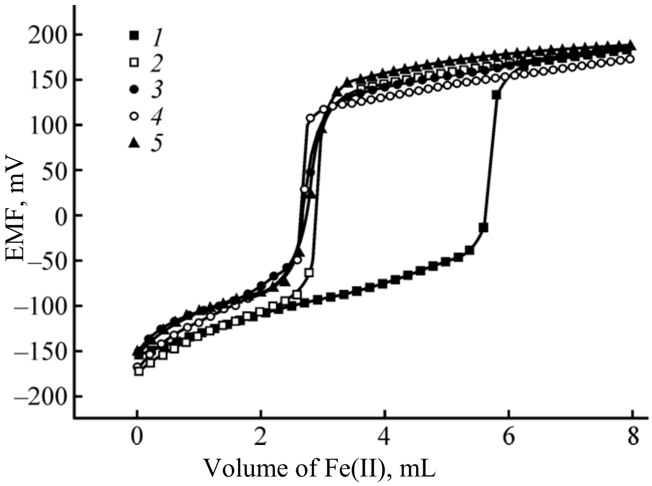

Fig. 10. Potentiometric measurements of class *a* metals ions over Pt electrode using $[Fe^{III}EDTA]^{-}$–$[Fe^{II}EDTA]^{2-}$ redox couple. (*1*) Blank, (*2*) Al^{3+}, (*3*) Ni^{2+}, (*4*) Cu^{2+}, and (*5*) Pb^{2+}.

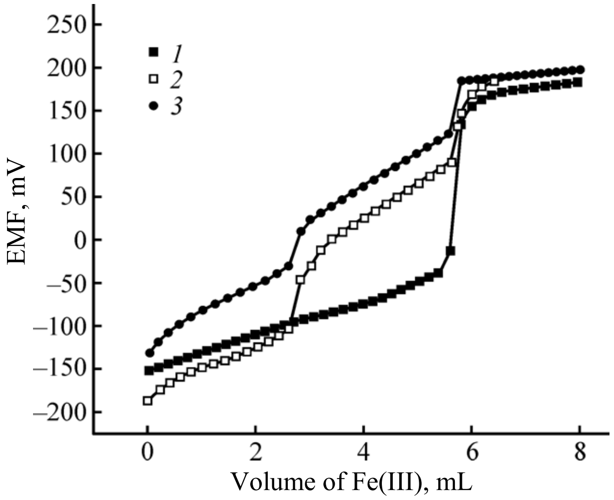

Fig. 11. Potentiometric measurements of class *b* metal ions over Pt electrode using $[Fe^{III}EDTA]^{-}$–$[Fe^{II}EDTA]^{2-}$ redox couple. (*1*) Blank, (*2*) Zn^{2+}, and (*3*) Cd^{2+}.

A distinctive feature of this method was simultaneous determination of the binary transition metal ions mixtures which was impossible with ion selective electrodes. The binary mixtures of transition metal ions were made by choosing metals from the categories *a*: non exchanging bound EDTA and *b*: exchanging bound EDTA. The potentiometric titration plot of binary mixture (Fig. 13) displayed two equivalence points. The first one was related with free EDTA solution and used as the indicator of the total molar amounts of both metals. The second equivalence point corresponded to exchange of bound EDTA between the metals ions.

The potential measured by platinum electrode in such titration is depicted by following equations [Eqs. (6), (7)]:

$$E_{\mathrm{Pt}} = E^0 \left[\frac{\mathrm{Fe^{III}(EDTA)^-}}{\mathrm{Fe^{II}(EDTA)^{2-}}}\right] - \frac{RT}{nF}\ln\frac{[\mathrm{Fe^{II}(EDTA)}]^{2-}}{[\mathrm{Fe^{III}(EDTA)}]^-} \quad (6)$$

or

$$E_{\mathrm{Pt}} = 0.13 - 0.059\log\frac{[\mathrm{Fe^{II}(EDTA)}]^{2-}}{[\mathrm{Fe^{III}(EDTA)}]^-}. \quad (7)$$

It was determined that 1 mL (0.001M) of Fe(II) solution and pH 4.2 were optimum conditions for analytical measurements [24].

Solvent coordination and ion pair formation for expansion in copper redox analysis window. The extent of redoximetric analysis of a reagent is limited by its redox potential [25]. Increase in redox potential of a reagent makes possible estimation of other systems of the reagent which could not be analysed otherwise owing to its low redox potential. This promotes oxidation of bigger number of systems than expected. This has been referred to as "expansion of copper redoximetric analysis window" (Scheme 5).

Cu(II)–Cu(I) aqueous medium redox potential is 0.153 V [15]. In acetonitrile media in presence of perchlorate anions Cu(II)–Cu(I) redox potential is 1.20 V [26]. This increase in copper redox potential has been attributed to the synergetic effect of acetonitrile and perchlorate ion on the redox couple and explained in terms of relative stabilization of oxidation states. Acetonitrile as a non-ionic donor type

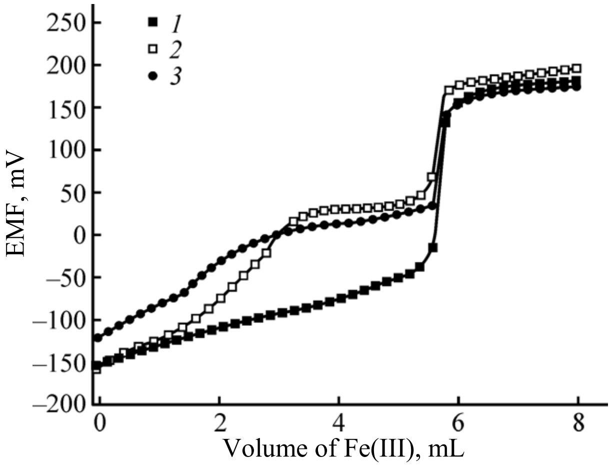

Fig. 12. Potentiometric estimation of class c metal ions over Platinum electrode using $[Fe^{III}EDTA]^{-}$–$[Fe^{II}EDTA]^{2-}$ redox couple: (*1*) blank, (*2*) Mg^{2+}, and (*3*) Ca^{2+}.

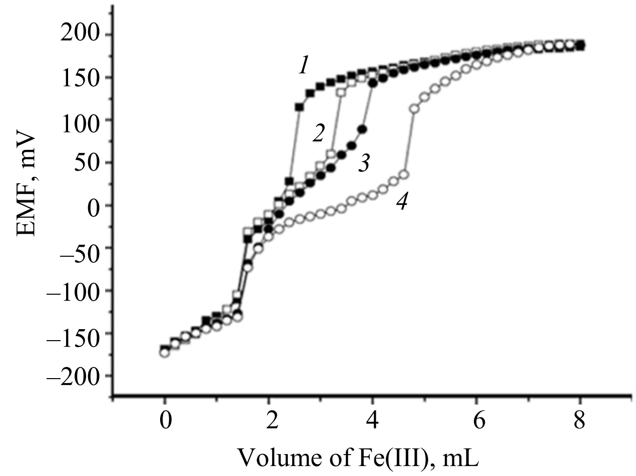

Fig. 13. Potentiometric estimation of varying amounts of binary metal ion mixture (Zn^{2+} and Ni^{2+}) over Platinum electrode using $[Fe^{III}EDTA]^{-}$–$[Fe^{II}EDTA]^{2-}$ redox couple. (*1*) 0.5 mL Zn^{2+} + 2.0 mL Ni^{+2}; (*2*) 1.0 mL Zn^{2+} + 1.5 mL Ni^{+2}; (*3*) 1.5 mL Zn^{2+} + 1.0 mL Ni^{+2}; (*4*) 2.0 mL Zn^{2+} + 0.5 mL Ni^{+2}.

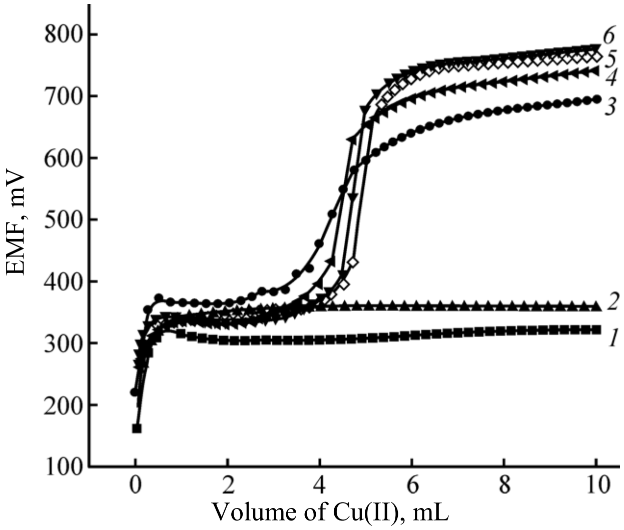

Fig. 14. Effect of acetonitrile and perchlorate ion concentration on potentiometric measurement of coordinated thiourea in $[Cu_2(Tu)_6]SO_4{\cdot}2H_2O$ by Cu(II). (*1*) $Cu(II)_{aq}$, (*2*) $Cu(II)_{aq}$ + 1.0 M ClO_4^-, (*3*) $Cu(II)_{AN}$, (*4*) $Cu(II)_{AN}$ + 0.05 M ClO_4^-, (*5*) $Cu(II)_{AN}$ + 0.15 M ClO_4^-, and (*3*) $Cu(II)_{AN}$ + 0.45 M ClO_4^-.

solvent stabilizes Cu(I) more than Cu(II). The effect is credited to the dominating tetrahedral geometry of $[Cu^I(MeCN)_4]^+$, the soft-soft interaction and π donor acceptor characteristics. High stability of Cu(I) in acetonitrile is supported by disproportionation constant of the reaction $2Cu^+ \rightarrow Cu^{2+} + Cu(s.)$ ($\log KD_{aq} = 6.26$ and $\log KD_{AN} = -20.8$) [27]. Negative value and low magnitude of the constant emphasizes high stability of Cu(I) in acetonitrile. The effect of perchlorate ions has been attributed to the kinetics of redox reaction and solvent dynamics. The polarizable perchlorate ion leads to formation of the ions pair [28] with the reacting complex ion which reduces the degree of solvation. Formation of the ion pair leads to lower solvolysis energy of the precursor complex thereby minimizing the activation barrier for the electron transfer. Based on this synergistic effect, Masood and coworkers [29] proposed an electroanalytical method for probing the composition of Cu(I) thiourea complexes via oxidation of coordinated thiourea by Cu(II) perchlorate in acetonitrile medium (Fig. 14). It predicts no reaction (potential change) in aqueous phase and an increasing potential change with increasing perchlorate ion concentration in acetonitrile media.

Scheme 5. Expansion of copper redoximetric analysis window.

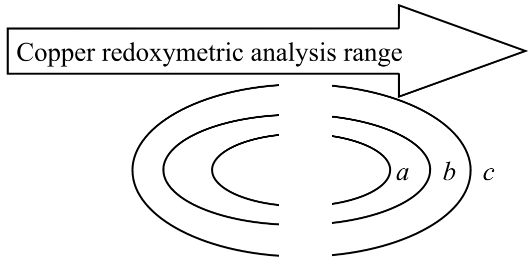

a: Cu^{II}/Cu^{I} redox potential in H_2O
b: Cu^{II}/Cu^{I} redox potential in CH_3CN
c: Cu^{II}/Cu^{I} redox potential in $CH_3CN + ClO_4^-$

Coordination modulated redox potentials: a novel approach to preventing oxidative stress. In biology transition metals work two ways, when coordinated to natural ligands they perform the desired job and if freed they bring the deleterious functions. Transition metals like iron and copper present a paradox in the context of biological oxygen chemistry, on one hand their complexes with bio-ligands are vital for cellular functions and on the other these in their free and electronically reduced state catalyze the harmful oxidation of biomolecules (DNA, proteins and lipids) [30] leading to harmful biological consequences. The transition metals [Fe(II) and Cu(II)] mediate oxidation of biomolecules that proceed via generation of reactive oxygen species (ROS) like the superoxide ($O_2^{\cdot-}$), hydroxyl ($OH^{\cdot}$) and hydroperoxyl

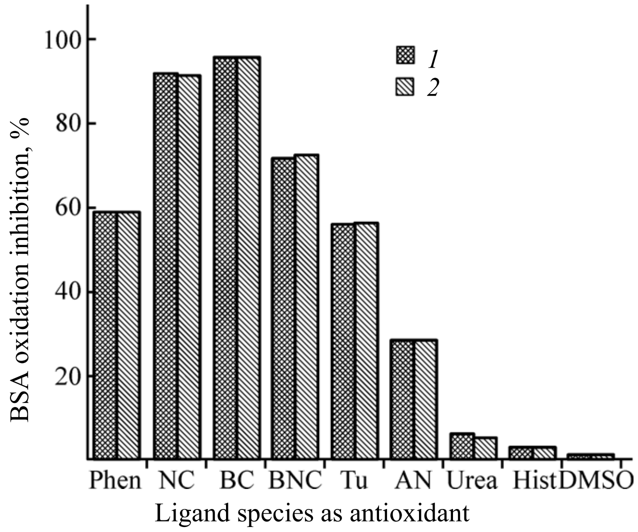

Fig. 15. Inhibition of BSA oxidation (%) by (*1*) Cu(II)–acetate and (*2*) Cu(II)–H_2O_2, in presence of Cu(I) stabilizing ligands.

($OOH^{\cdot}$) radicals [30]. Generation of free radicals is linked to the redox potential of transition metals. The redox status of cells is determined mostly by iron (and sometimes copper) redox couples and retained within strict physiological margins through homeostasis ensuring no free intracellular Fe(II). However, under stress conditions the generated excess of $O_2^{\cdot-}$ leads to release of Fe(II) from iron containing [4Fe–4S] molecules. Released Fe(II) participates in the Fenton reaction, generating highly reactive hydroxyl radical [31]:

$$Fe^{II} + H_2O_2 \rightarrow Fe^{III} + OH^{\cdot} + OH^{-}. \qquad (8)$$

Fe(III) produced is reduced back by superoxide radical to Fe(II):

$$Fe^{III} + O_2^{\cdot-} \rightarrow Fe^{II} + O_2. \qquad (9)$$

Generally, the reduced state of any transition metal, depending on its redox potential, can undergo the Fenton reaction producing ROS like the hydroxyl radicals [31]:

$$M^{n+} + H_2O_2 \rightarrow M^{(n+1)} + OH^{\cdot} + OH^{-}, \qquad (10)$$

$$M^{n+} = Cu^{+}, Cu^{2+}, Ti^{3+}, Co^{2+}.$$

Selective chelation of transition metals ions modifies their redox potential and can prevent the ions participation in the catalytic processes producing reactive oxygen species, (ROS). Hence, designed chelation can block such unwanted biological oxidation and help to prevent oxidative stress [32]. Coordination modified redox potentials, thus, can be a

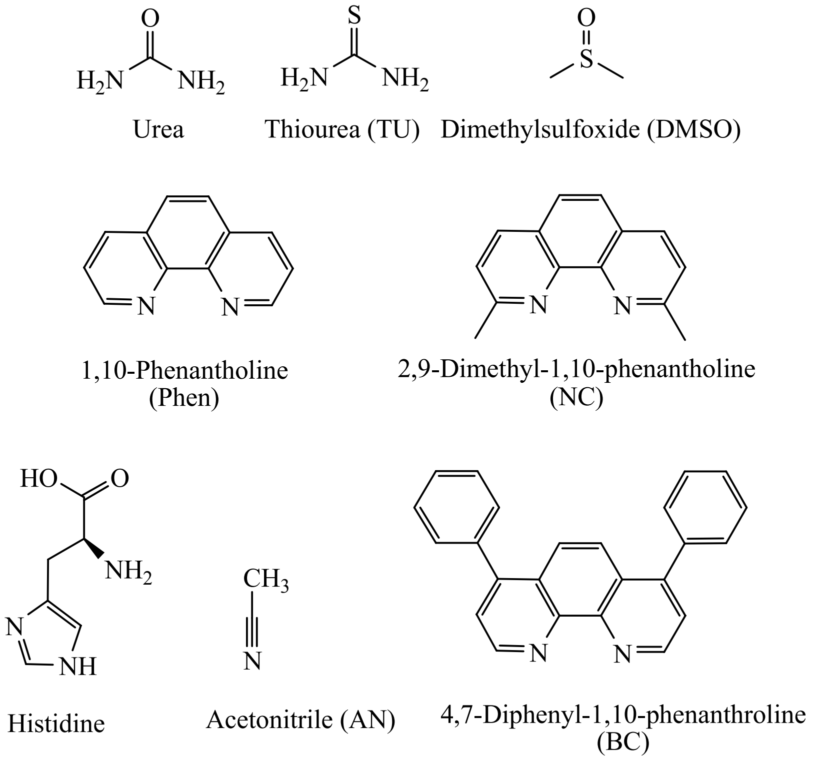

Fig. 16. Structures of the studied Cu(I) stabilizing ligands.

novel method in prevention of oxidative stress [33]. The distinctive feature of this approach is the fact that, while other antioxidant systems work passively by preventing the damage of ROS via their radical scavenging ability, the new approach is based on active blocking of ROS generation. The chelates that stabilize Fe(II)(Phen, Bipy) increase the redox potential of iron and inhibit its oxidation to Fe(III). Similarly the chelates that stabilize Cu(I) inhibit its oxidation to Cu(II) and block formation of ROS. Raashid and coworkers [34] studied the comparative inhibitory effect of different ligands on oxidation of protein Bovine Serum Albumin (BSA) by Cu(II) hydrogen peroxide and Cu(II) acetate oxidizing systems. Copper mediated oxidative damage to BSA was estimated by spectrophotometric quantification of protein carbonyl formation via measuring absorbance at 370 nm according to the Levine protocol [35]. Efficiency of studied ligands in prevention of BSA oxidation by Cu(II)acetate and Cu(II)peroxide is presented in Fig. 15.

The relative action of the studied ligands on BSA oxidation is explained in terms of their propensity to stabilize Cu(I) oxidation state (Fig. 16).

Ability of the ligands to stabilize Cu(I) originates from their soft-soft interaction, preferred tetrahedral geometry and degree of π back acceptance. Higher activity of thiourea compared to that of urea is due to soft-soft interaction between Cu(I) and sulphur donor site of the TU ligand. Among 1,10-phenanthroline (Phen) and 2,9-dimethyl-1,10-phenanthroline (NC) higher ability of NC is due to its tendency to form tetrahedral Cu(I) complex. Between 4,7-diphenyl-1,10-phenanthroline (BC) and Phen higher ability of the latter to stabilize Cu(I) is due to enhanced π back acceptance of BC over the Phen ligand.

Scheme 6. Siderophore mediated transport of iron to a microbial cell.

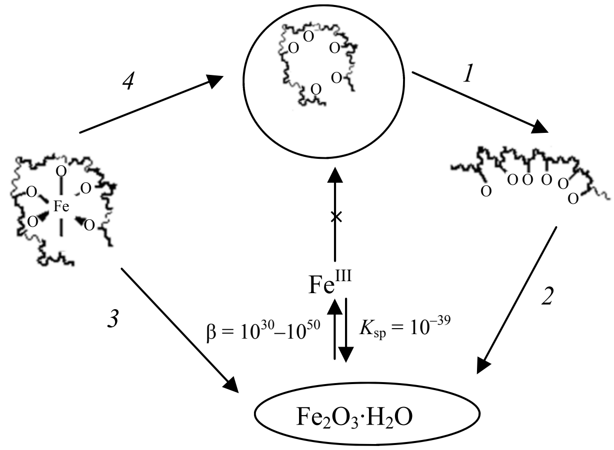

Chelation: the vehicle for iron transport in biological systems. Availability of iron in nature is limited by its extremely facile hydrolysis reaction ($K_{sp} \sim 10^{39}$) forming insoluble hydrated oxides $Fe_2O_3·6H_2O$ under natural pH conditions. Living organisms have evolved with mechanisms to acquire this abundant yet scarcely bioavailable vital metal for supporting life processes [36, 37].

Chelation is one of the finest processes by which microbes solubilize iron from its hydrated oxide deposits. Organisms have the ability to produce small chelating molecules called siderophores for specific sequestering of iron in the presence of other metals. Siderophores dissolve iron from its deposits due to their high thermodynamic affinity (formation constant) for binding Fe(III). The siderophore chelated Fe(III) is soluble, does not hydrolyze or precipitate and facilitates specific recognition and uptake of the metal at the cells surface [38].

Siderophore mediated iron acquisition by microbes can be illustrated by Scheme 6 according to which a cell synthesizes and releases a polydentate chelating ligand called siderophore (*1*). The siderophore leaches out insoluble iron from its deposits by selective chelation (*2*). Fe(III) siderophore chelate diffuses back to the cell (*3*) where it is recognized by a cell receptor (*4*) and iron is released via the metabolic processes within the cell [39] .

As a carrier molecule of iron, siderophore has to extract iron efficiently from its insoluble sediments and at the same time easily liberate the bound iron within the cell. High stability constant of iron siderophore complexes guarantee the efficient leaching but also raise the concern of iron release by the cell [40, 41]. Three mechanisms have been proposed for the release of iron from its thermodynamically stable siderophore complex: (1) Hydrolysis of the siderophore; (2) proton assisted dissociation of the complex; (3) reduction of the metal center [36, 42].

The redox mechanism of iron release from siderophore proposes reduction of Fe(III) metal centre by means of *in vivo* reducing agents, including small molecule reducing agents in cytosol and also reductase enzymes. Reduction promotes release of iron from the iron-siderophore complex [43]. Reduction of iron, from Fe(III) to Fe(II), diminishes its charge density

Scheme 7. Fe(III) chelation Siderophores

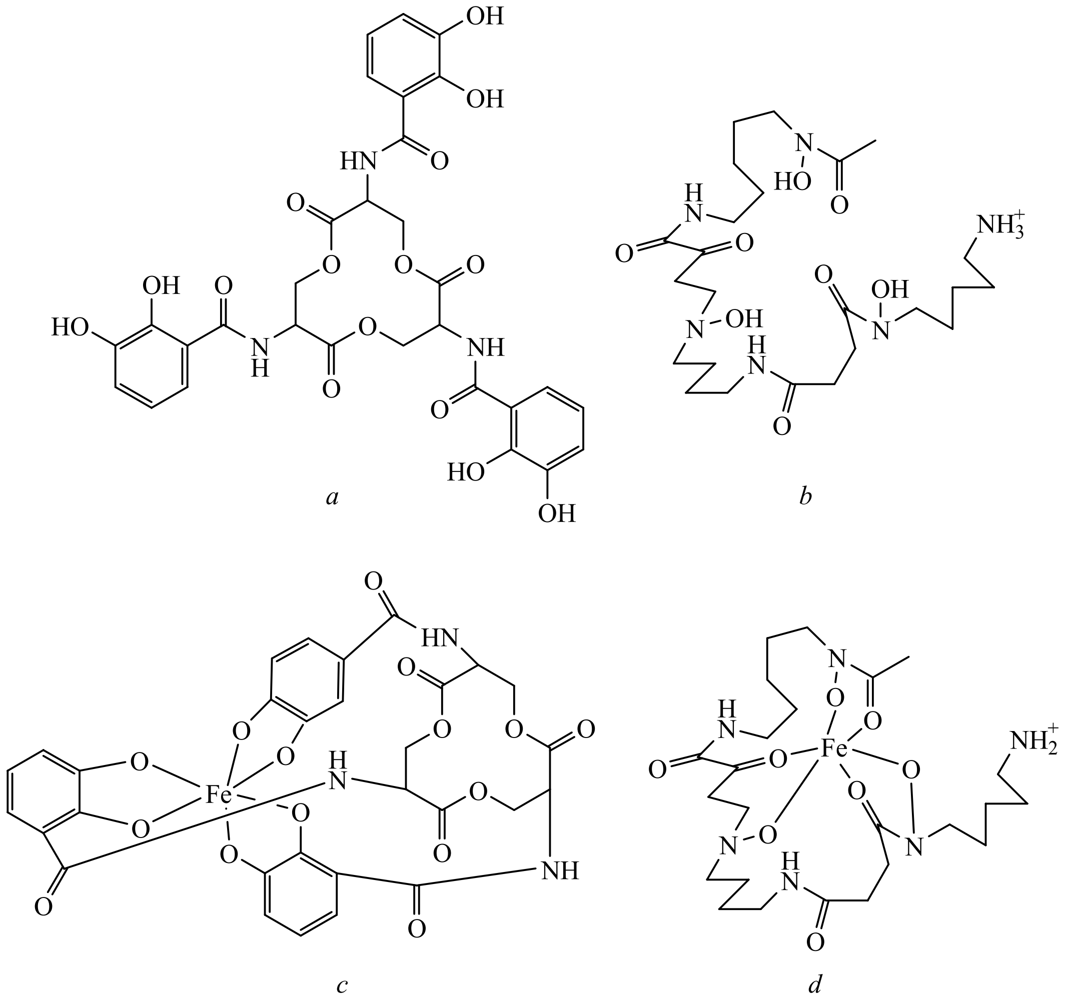

and converts iron from a hard to a border-line hard/soft Lewis acid, decreasing its affinity for the hard negatively charged oxygen donors of the siderophores. Reduction of Fe(III) to Fe(II) thus facilitates its release by decreasing thermodynamic stability of iron siderophore complex and enhancing kinetics of the ligand exchange [44, 45] (Scheme 7).

The siderophores are microbially synthesized low molecular weight chelators of Fe(III) that usually involve bidentate catechol type (a) or hydroxamic acid type (b) donor groups. Such chelators posses a very strong binding affinity for Fe(III) {enterobactin (c) log $\beta Fe^{III} = 49$, desferriox- amine B (d) log $\beta Fe^{III} = 30.6$} [39]. Redox potentials of Fe(III) siderophore complexes are often too negative to allow reduction of Fe(III) by available biological reducing agents. The effect of coordination inspired redox process in release of iron from highly stable Fe(III) siderophore complex was proposed by Mies and coworkers [46]. The redox potential shift was due to formation of a ternary complex between Fe(III) siderophore and Fe(II) chelating ligand. Formation of the ternary complex shifted iron redox potential towards more positive value due to the increased stabilization of Fe(II) afforded by mixed donor characteristics of the coordination sphere. The shift in iron redox potentials has been presented as a function of Fe(II) affinity to a ligand and concentration of the competing Fe(II) chelator. Higher concentration of Fe(II) chelator shifted the competing equilibria favoring reduction of Fe(III) to Fe(II) [Eqs. (11)–(14)].

$$Fe^{III}Sid + e^{-} \rightarrow Fe^{II}Sid, \qquad (11)$$

$$Fe^{II}Sid \rightarrow Fe^{II} + Sid, \qquad (12)$$

$$Fe^{II} + L \rightarrow Fe^{II}L, \qquad (13)$$

$$E_{\mathrm{rxn}} = E_{\mathrm{red}}^{\mathrm{Fe(III)Sid}} + \frac{0.0592}{n}\log\left(1 + \frac{K^{\mathrm{Fe(II)L}}[\mathrm{L}]}{K^{\mathrm{Fe(III)Sid}}[\mathrm{Sid}]}\right). \quad (14)$$

Here equations represent reduction of Fe(III) sidero-phore complex [Eq. (11)], release of Fe(II) from sidero-phore [Eq. (12)], chelation of Fe(II) with a competing Fe(II) chelator [Eq. (13)] and a net reaction describing the redox potential of a coupled electron transfer complexation reaction [Eq. (14)].

According to Eq. (14), the stronger Fe(II) chelators {higher $K\mathrm{Fe^{II}L}$} and higher competing chelator concentration increase iron redox potential, favoring reduction of Fe(III) to Fe(II). This coordination modulated shift brings the redox potential of iron-siderophore complexes into the range of biological reductants. Mies and co-authors [46] validated the coupled equilibria concept involving ternary complex formation of Fe(III) siderophore with Fe(II) chelating ligand by investigating the effect of sulfonated bathophenanthroline (BPDS) ligand on release of Fe(III) from the desferrioxamine B complex catalyzed by glutathione and ascorbic acid. In the spectro-photometric study without BPDS no reduction and removal of iron from the siderophore was observed. Addition of BPDS facilitated removal of iron from the complex due to formation of the Fe(II)–BPDS complex. The ternary complex (Fig. 17) was proposed to be formed between Fe(III), desferrioxamine B and BPDS [46].

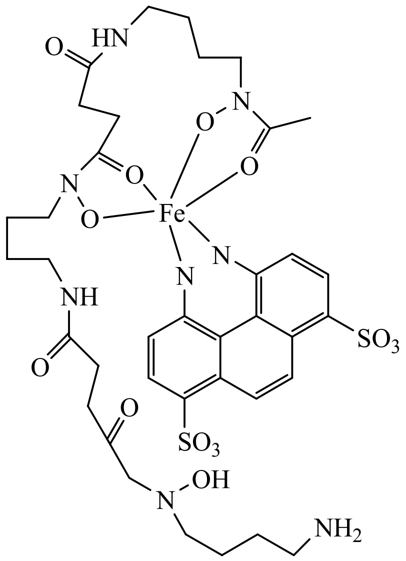

Fig. 17. Structure of the proposed ternary complex between Fe(III), desferrioxamine B and BPDS.

Coordination modified iron redox potential utilized in environmental nitro aromatic reduction. Nitro aromatic compounds (NACs) are wide-spread aquatic contaminants from pesticide and industrial sources. Reducing a toxic contaminant to relatively less toxic form is the important process for environmental toxicology. Dissolved Fe(II) species are capable of reducing organic contaminants like carbamoyloxime pesticides [47]. The direct reduction of NACs by Fe(II) is often painfully slow [48]. Chelating ligands enhance the rate of reduction of contaminants by dissolved Fe(II). This can be attributed to modification in Fe(III)–Fe(II) reduction potential on complexation with organic ligands [6–9, 49].

Strathmann and coauthors [47] studied abiotic reduction of nitro aromatic compounds by aqueous Fe(II)−catechol complexes. The proposed mechanism involves three two electrons steps as presented in Fig. 18.

On the bases of experimental data it was deduced that complexes that stabilized Fe(III) and lowered the reduction potential of Fe(III)–Fe(II) redox couple were more efficient for nitro aromatic reduction. It was suggested that the propensity of iron complexes for reduction of nitro aromatic compounds originated from

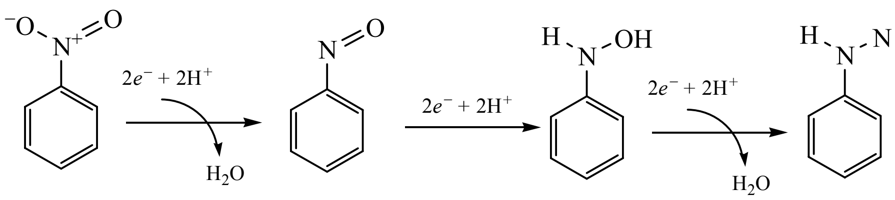

I NB **II** NsB **III** HA **IV** An

Fig. 18. The proposed mechanism of nitro aromatic compounds reduction to aniline in presence of Fe(II) complexes with organic ligands [50]. (NB) Nitrobenzene, (NsB) nitroso benzene, (HA) hydroxylamine, (An) aniline An.

their ability to decrease the redox potential of Fe(III)–Fe(II) redox couple. Increase in the redox potential of Fe(III)–Fe(II) couple increased the reaction halftime of nitro aromatic abiotic reduction by thiols. Considering the cysteine as the basic organothiol ligand, Naka and coauthors [50] worked out the structure activity relationship among different thiol systems for nitro aromatic reduction. Activity of iron complexes in nitro aromatic reduction was due to Fe(III) stabilization and low Fe(III)–Fe(II) redox potential.

CONCLUSIONS

In summary, this work presents the review of the complexation effect on redox potential of transition metal systems. The relative stabilization of transition metals oxidation states in a redox couple tunes the complexed state redox potential both ways from its uncomplexed state redox potential. The ligand tuned redox potentials are explored in the design and development of redox systems for novel analytical applications. The studies of potentiometeric applications based on ligand modulated redox activity of iron, cobalt and copper containing systems in presence of 1,10-phenanthroline and neocuproine ligands are highlighted. Coordination modified redox potentials of transition metals with selected ligands is a novel approach to prevention of oxidative stress, iron assimilation by siderophores and natural attenuation of the toxic environmental contaminants (nitro aromatics).

REFERENCES

1. Song, W., Chen, Z., Brennaman, M.K., Concepcion, J.J., Otavio, A., Patrocinio, T., Murakami, N.Y., and Meyer, T.J., *Pure and Applied Chemistry,* 2011, vol. 83, p. 749. DOI: 10.1351/PAC-CON-10-11-09.
2. Kashif, M.K., Axelson, J.C., Duffy, N.W., Forsyth, C.M., Chang, C.J., Long, J.R., Spiccia, L., and Bach, U., *J. Am. Chem. Soc.*, 2012, vol. 134, p. 16646. DOI: 10.1021/ja305897k.
3. Reisner, E., Arion, V.B., Fatima, M., da Silva, C.G., Lichtenecker, R., Eixhinger, A., Keppler, B.K., Kukushkin, V.Y., and Pombeiro, A.J.L., *Inorg. Chem.,* 2004, vol. 43, p.7083. DOI: 10.1021/ic049479c.
4. Marshall, N.M., Garner, D.K., Wilson, T.D., Gao, Y.G., Robinson, H, Nilges, M.J., and Lu, Y., *Nature,* 2009, vol. 462, p. 113. DOI: 10.1038/nature08551.
5. Zuris, J.A., Halim, D.A., Conlan, A.R., Abresch, E.C., Nechushtai, R., Paddock, M.L., and Jennings, P.A., *J. Am. Chem. Soc.,* 2010, vol. 132, p. 13120. DOI: 10.1021/ja103920k.
6. Teshima, N., Katsumata, H., and Kawashima, T., *Anal. Sci.,* 2000, vol. 16, p. 901 DOI: 10.2116/analsci.16.901.
7. Rizvi, M.A., Syed, R.M., and Khan, B.U., *J. Chem. Educ.,* 2011, vol. 88, p. 220. DOI: 10.1021/ed100339g.
8. Rizvi, M.A., Teshima, N., and Peerzada, G.M., *Croat. Chem. Acta,* 2013, vol. 86, p. 345. DOI: 10.5562/cca2167.
9. Buerge, I.J. and Hug, S.J., *Environ. Sci. Tech.*, 1998, vol. 32, p. 2092, DOI: 10.1021/es970932b.
10. Boukhalfa, H., and Crumbliss, A.L., *Biometals*, 2002, vol. 15, p. 325 DOI: 10.1023/A:1020218608266.
11. Mailloux, R.J., Jin, X., and Willmore, W.G., *Redox Biol.*, 2014, vol. 2, p. 123.
12. Ibanez,J. G., Gonzalez, I., and Cardenas, M.A., *J. Chem. Educ.* 1988, vol. 65: p. 173. DOI: 10.1021/ed065p173.
13. Rizvi, M.A., Raashid, M., Jan, R., and Peerzada, G.M., *Chem. Ed.,* 2011, vol. 16, p. 72. DOI 10.1333/s00897112337a.
14. McBryde,W.A.E., *A Critical Review of Equilibrium Data for Proton and Metal Complexes of 1,10-Phenanthroline, 2,2-Bipyridyl and Related Compounds*, Oxford: Pergamon, 1975.
15. David, R.L., *Handbook of Chemistry and Physics*, New York, CRC Press Taylor & Francis, 2005–2006, pp. 8–21.
16. Ogura, K., Urabe, H., and Yosino, T. *Electrochim. Acta*, 1977, vol. 22, p. 285. DOI: 10.1016/0013-4686(77)85074-3.
17. Raashid, S., Rizvi, M.A., and Khan, B.U., *J. Pharm. Res.,* 2012, vol. 5, p. 2715.
18. Teshima, N. and Kawashima, T., *Bull. Chem. Soc. Jpn,* 1996, vol. 69, p. 1975 DOI: 10.1246/bcsj.69.1975.
19. Huang, W.Q., Huang, G.F., Wang, L.L and Shi, X.G., *Int. J. Electrochem. Sci.*, 2008, vol. 3, p. 1316.
20. Rizvi, M.A., Akhoon, S., Maqsood, S.R., and Peerzada, G.M., *Croat. Chem. Acta,* 2015, vol. 88 (in press); http://dx.doi.org/10.5562/cca2479.
21. Maqsood, S.R., Bhat, M.A., and Khan, B.U., *J. Coord. Chem.,* 2013, vol. 66, p. 1211 DOI: 10.1080/00958972.2013.778987.
22. Gupta, V.K., Goyal, R.N., Khayat, M.A., Kumar, P., and Bachheti, N., *Talanta,* 2006, vol. 69, p. 1149. DOI: 10.1016/j.talanta.2005.12.040.
23. Raashid, S., Chatt, O. A., Rizvi, M.A., Bhat, M.A., and Khan, B.U., *Talanta,* 2012, vol. 101, p. 246. DOI: 10.1016/j.talanta.2012.09.020.
24. Rizvi, M.A., Teshima, N., and Peerzada, G.M., *Asian J. Chem.,* 2013, vol. 25, p. 4776. DOI: 10.14233/ajchem.2013.14099 .
25. Serjeant, E.P., *Potentiometry and Potentiometric Titrations. In A Series of Monographs on Analytical Chemistry and Its Applications*, Vol. 69, Elving, P.J. and Winefordner, J.D., Eds., New York: John Wiley & Sons, 1984, p. 38.

26. Namazian, M., Lin, C.Y., and Coote, M.L., *J. Chem. Theo. Comput.*, 2010, vol. 6, p. 2721. DOI: 10.1021/ct1003252.
27. Ahrland, S., *Pure Appl. Chem.*, 1982, vol. 54, p. 1451 10.1351/pac198254081451.
28. Li, T and Balbuena, P. B., *J. Electrochem. Soc.,* 1999, vol. 146, p. 3613 DOI: 10.1149/1.1392523.
29. Rizvi, M.A., Akhoon, S., Maqsood, S.R., and Peerzada, G.M., *J. Anal. Chem.,* 2015, vol. 70, p. 632. DOI: 10.1134/S1061934815050093.
30. Aust Koppenol, W.H., *Oxidative Damage and Repair: Chemical, Biological and Medical Aspects* Oxford, England, Pergamon Press, 1991, p. 802.
31. Kosman, D.J., *Coord. Chem. Rev.*, 2013, vol. 257, p. 210. DOI: 10.1016/j.ccr.2012.06.030.
32. Zhu, B.-Z., Antholine, W.E., Frei, B., *Free Rad. Biol. Med.*, 2002, vol. 32, p. 1333. DOI: 10.1016/S0891-5849(02)00847-X.
33. Milaeva, E.R., *Curr. Top. Med. Chem*, 2011, vol. 11, p. 2703. DOI: 10.2174/156802611798040741.
34. Maqsood, S. R., *PhD Thesis (Chemistry)*, University of Kashmir, India, 2013
35. Levine R.L., Williams J, Stadtman, E.R., and Shacter, E., *Methods Enzymol.,* 1994, vol. 233, p. 346. DOI: 10.1016/S0076-6879(94)33040-9.
36. Albrecht, A.M. and Crumbliss, A.L., *Met. Ions Biol. Syst.,* 1998, vol. 35, p. 239.
37. Kalinowski, D.S. and Richardson, D.R., *Pharmacol. Rev.,* 2005, vol. 57, p. 547. DOI: 10.1124/pr.57.4.2.
38. Crumbliss, A.L. and Harrington, J.M., *Adv. Inorg. Chem.*, 2009, vol. 61, p. 179. DOI: 10.1016/S0898-8838(09)00204-9.
39. Liu, Z.D. and Hider, R.C., *Coord. Chem. Rev.,* 2002, vol. 232, p. 151. DOI: 10.1016/S0010-8545(02)00050-4.
40. Dhungana, S., Anderson, D.S., Mietzner, T.A., and Crumbliss, A.L., *Biochemistry*, 2005, vol. 44, p. 9606. DOI: 10.1021/bi0505518
41. Dhungana, S., Anderson, D.S., Mietzner, T. A., and Crumbliss, A.L., *J. Inorg. Biochem*., 2004, vol. 98, p. 1975. DOI: 10.1016/j.jinorgbio.2004.08.00442.
42. Dhungana, S. and Crumbliss, A.L., *Geomicrobiology,* 2005, 22, p. 87. DOI: 10.1080/01490450590945870.
43. Harrington, J.M., and Crumbliss, A.L., *Biometals,* 2009, vol. 22, p. 679. DOI: 10.1007/s10534-009-9233-4.
44. Raymond, K.N. and Dertz, E.A., in *Iron Transport in Bacteria*, Crosa, J.H., Rey, A.R., and Payne, S.M., Eds., Washinington, DC, ASM Press , 2004, pp. 3–17.
45. Richens, D.T., *Chem Rev* , 2005, vol. 105, p. 1961. DOI: 10.1021/cr030705u.
46. Mies, K.A., Wirgau, J.I., and Crumbliss, A.L., *Biometals*, 2006, vol. 19, p. 115. DOI: 10.1007/s10534-005-4342-1.
47. Strathmann, T.J. and Stone, A.T., *Environ Sci. Tech.,* 2002, vol. 36, p. 5172. DOI: 10.1021/es0205939.
48. Bussan, A.L. and Strathmann, T.J., *Environ. Sci. Tech.*, 2007, vol. 41, p. 6740. DOI: 10.1021/es071108i
49. Kim, D. and Strathmann, T.J., *Environ. Sci. Tech.*, 2007, vol. 41, p. 1257. DOI: 10.1021/es062365a.
50. Naka, D. and Kim, D., *Environ. Sci. Tech.,* 2006, vol. 40, p. 3006. DOI: 10.1021/es060044t .